Supplementary Information

Modular construction of mammalian gene circuits using TALE transcriptional repressors

Yinqing Li[1,6], Yun Jiang[2,6], He Chen[2,6], Weixi Liao[2,3], Zhihua Li[4], Ron Weiss[1,5,*] and Zhen Xie[2,3,*]

[1]Department of Electrical Engineering and Computer Science, Massachusetts Institute of Technology, 40 Ames St, Cambridge MA 02142, USA

[2]Bioinformatics Division/Center for Synthetic & Systems Biology, Tsinghua National Laboratory for Information Science and Technology, Tsinghua University, Beijing, 100084, China

[3]MOE Key Laboratory of Bioinformatics; Department of Automation, Tsinghua University, Beijing 100084, China

[4]Institute of Medical Biology, Chinese Academy of Medical Sciences and Peking Union Medical College, 935 Jiaoling Road, Kunming, Yunnan, 650118.

[5]Department of Biological Engineering, Massachusetts Institute of Technology, 40 Ames St, Cambridge MA 02142, USA

[6]These authors contribute equally to this work

* To whom correspondence should be addressed: E-mail: zhenxie@tsinghua.edu.cn (Z.X.) or rweiss@mit.edu (R.W.).

Supplementary Results

List of abbreviations

FACS: fluorescence activated cell sorting

EYFP: enhanced yellow fluorescent protein

mKate2: red fluorescent protein

iRFP: near-infrared fluorescent protein

EBFP2: enhanced blue fluorescent protein

TagBFP: monomeric blue fluorescent protein

CMV: cytomegalovirus immediate-early enhancer

hEF1α: human elongation factor 1α promoter

CAG: hybrid promoter combing CMV-IE promoter, chicken β-actin promoter, 5' flanking sequence and the first intron sequence with a modified splice acceptor sequence derived from the rabbit β-globin gene

TRE: tetracycline responsive element

rtTA: reverse tetracycline-controlled transactivator

Bla: Blasticidin resistance gene (blasticidin-S deaminase)

Gal4VP16: transcriptional activator that activates expression downstream of UAS sequence

2A: self-cleaving 2A peptides

NOS: transcription terminator derived from nopaline synthase gene from Agrobacterium tumefaciens

DMEM: Dulbecco's modified Eagle's medium

FBS: fetal bovine serum

HeLa: a cervical cancer cell line derived from cells taken from Henrietta Lacks

HEK293: human embryonic kidney 293 cell line

Supplementary Figures

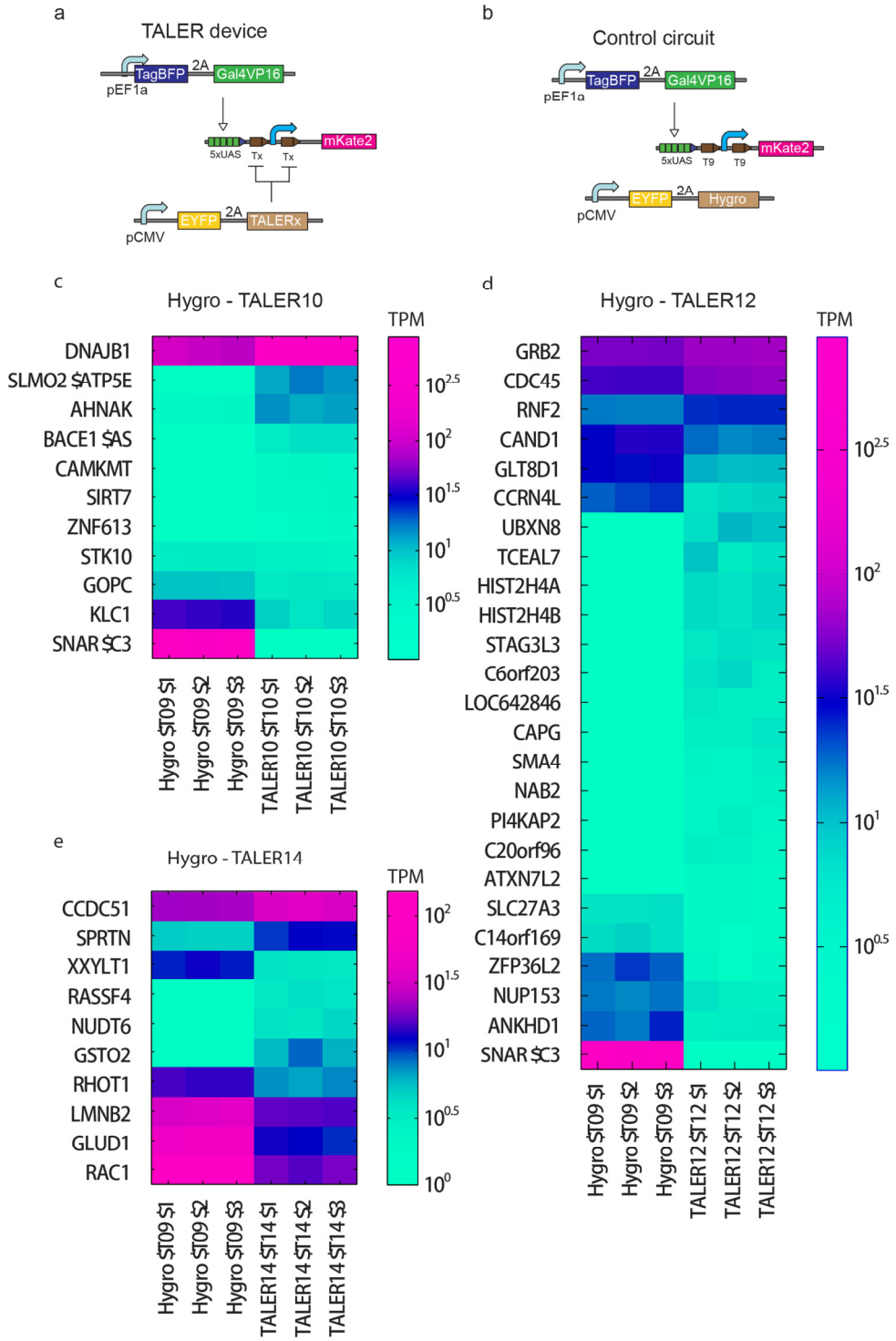

Supplementary Figure 1. RNA sequencing analysis of HEK293 cells transfected with TALER devices.

(a) Design of a TALER device used in RNA sequencing (RNA-seq). Tx: binding site for TALER x. Blue arrow represents a minimal CMV promoter. Lines with arrows indicate up-regulation and lines with bars indicate down-regulation. (b) Design of a control circuit used in RNA-seq. Hygro: hygromycin resistance gene. (c) - (e), On average, 9043 genes per sample were detected in the RNA-seq after filtering. Heat-maps show transcripts per million (TPM) of genes found differentially expressed when comparing RNA-seq results of control circuit to that of (c) TALER10 device, (d) TALER12 device, (e) TALER14 device. No differentially expressed genes were found for TALER9 device or TALER21 device. Row labels show name of differentially expressed genes and column labels show name of circuits transfected in each sample. Hygro-T09-1, -2, -3 represents three biological replicates transfected with the control circuit. TALERx-Tx-1, -2, -3 represents three biological replicates transfected with the TALERx (x = 10, 12 or 14) device.

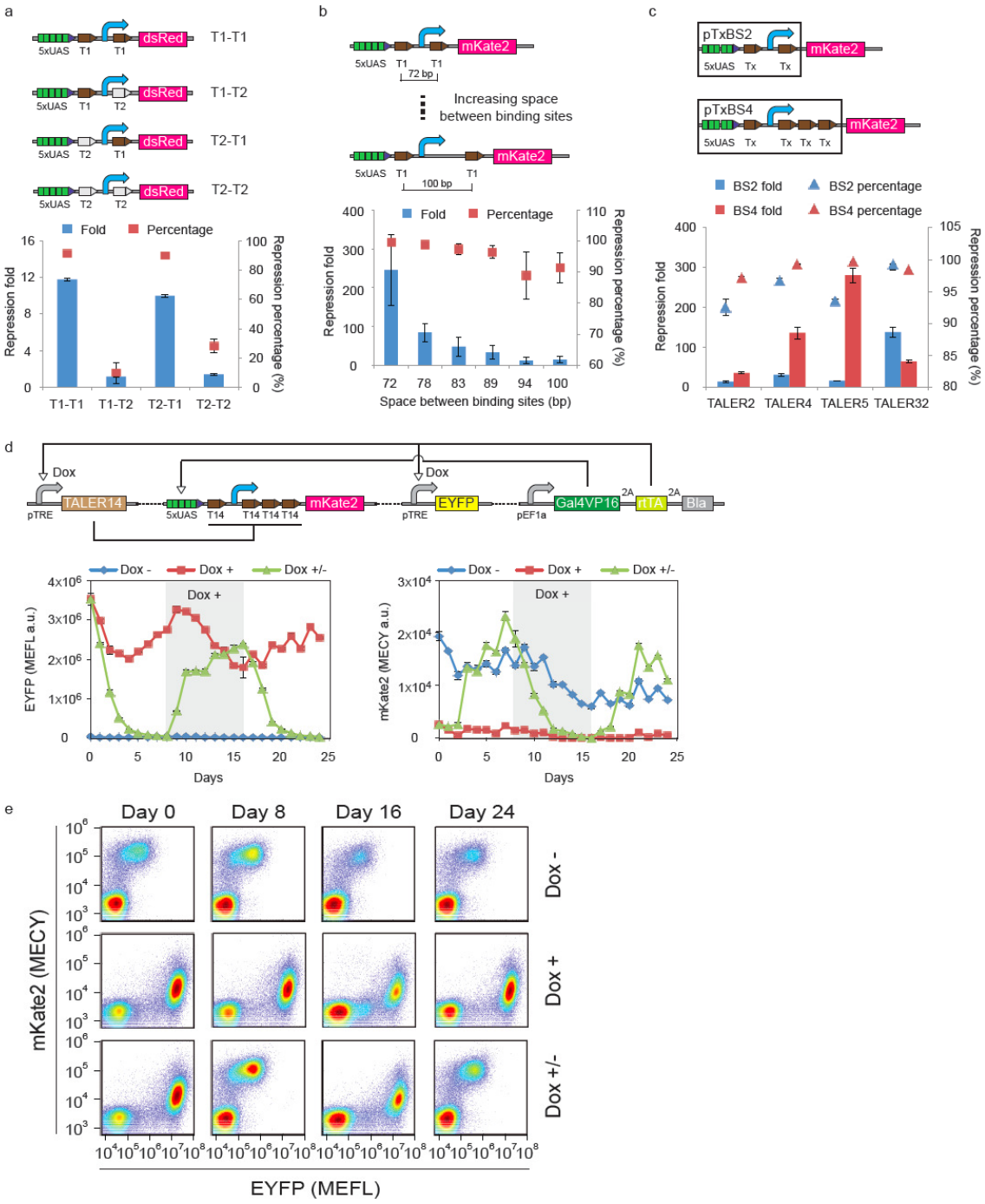

Supplementary Figure 2. Optimization of TALER promoter and TALER dynamics.

(a) TALER1 repression on variant promoters with T1 binding sites or T2 binding sites that serve as mock sequences. (b) TALER1 repression on variant promoters with indicated distances between upstream and downstream binding sites. (c) TALER repression on promoters with two (pTxBS2) or four binding sites (pTxBS4). (d) and (e) Dynamics of TALER in an engineered stable cell line. (d) Schematic representation of a

TALER circuit integrated into the genome of HEK293 cells. Lines with arrows indicate up regulation and lines with bars indicate down regulation. Shaded region labeled with Dox+ represents the time window of 1 μg/mL Doxycycline in culture media for the treatment labeled with Dox+/-. Treatments labeled with Dox+ and Dox- represent cell populations with and without 1 μg/mL Doxycycline in culture media respectively during the time course of the experiment. (e) Representative beads normalized EYFP and mKate2 scatter plots are shown at indicated day with (+) or without (-) or alternatively adding or removing (+/-) 1 μg/mL doxycycline during the course of experiments. (a) to (d) Transfection configuration is described in Supplementary Table 2. Each data point shows mean ± SD from three independent flow cytometry experiments.

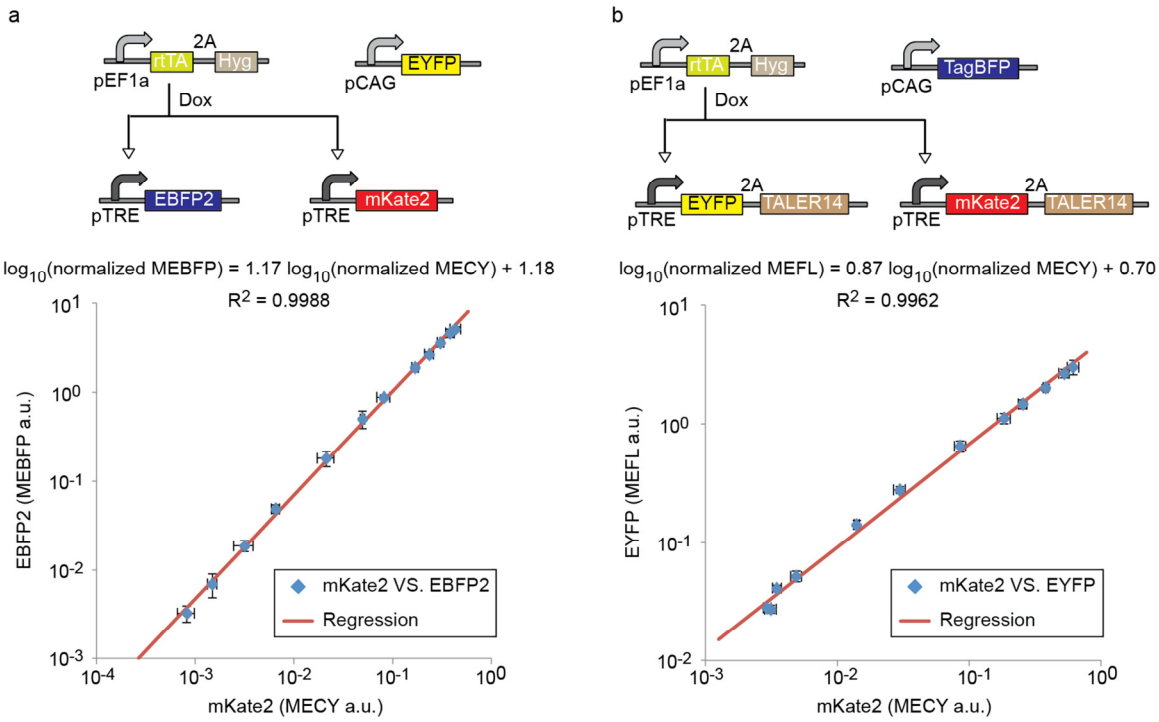

Supplementary Figure 3. Standardization of mKate2, EYFP, and EBFP2 channels

(a) Diagram of circuit used to establish EBFP2 and mKate2 conversion model. Correlation between beads normalized EBFP2 and mKate2 is shown in the bottom panel. Equation for linear regression is indicated above the correlation plot. (b) Diagram of circuit used in standardizing EYFP and mKate2 fused to TALER with a self-cleaving 2A linker. Correlation between beads standardized EYFP and mKate2 is shown in the bottom panel. Equation for linear regression is indicated above the correlation plot.

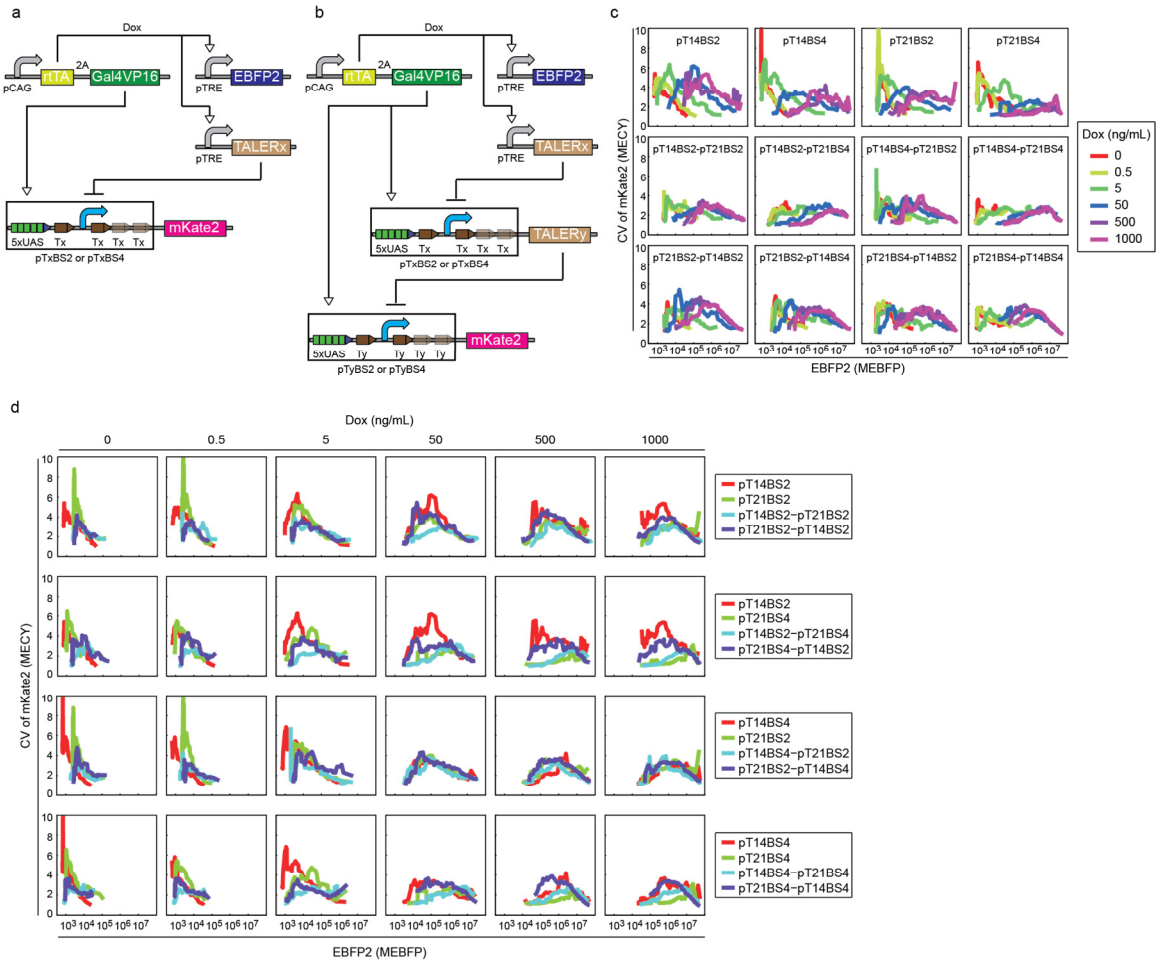

Supplementary Figure 4. Variance analysis of TALER devices and cascade circuits.

(a) Schematic representation of TALER devices. pTxBS2 and pTxBS4 are TALER promoters with two binding sites or four binding sites, respectively. (b) Schematic representation of TALER cascade circuit. For simplicity, pTxBS2 and pTxBS4 are depicted in the same diagram with two downstream binding sites in pTxBS4 promoter colored with reduced intensity. (c) and (d) Distributions of CV of individual TALER devices and cascades across the input range. For simplicity, six of fourteen tested Doxycycline concentrations are showed on the top of each panel. (c) Plots in the first row show the results of individual TALERs, and plots in the second and the third rows show the results of TALER cascades. (d) Plots in different rows indicate different TALER cascade and the corresponding constituents.

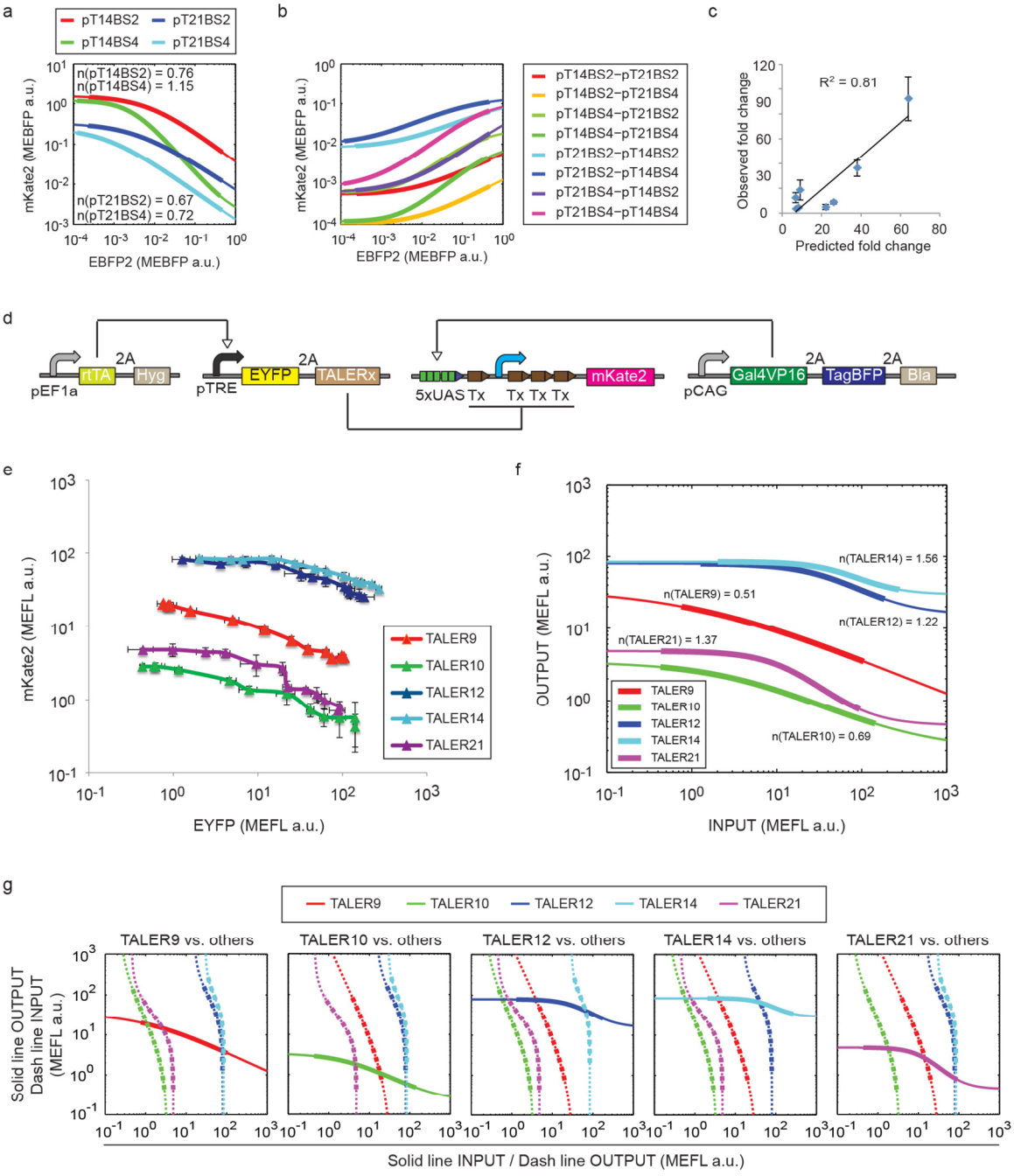

Supplementary Figure 5. Transfer function curve analysis of TALERs, TALER cascades and TALER switches.

(a) Computationally fitted transfer curves using Hill functions for data shown in Fig. 2. n(pTxBS2) or n(pTxBS4) indicate Hill coefficients. The thick region, and thin region of each curve represents experimentally observed input range and extrapolated values based on fitted function, respectively. The Hill coefficients range from 0.67 to 1.15. (b) Simulated cascade transfer curves based on the transfer curves of individual TALERs. (c)

Pearson correlation, calculated as R squared, between predicted and observed maximum fold changes of TALER cascades. (d) Schematic of circuits used for measuring transfer function curves of 2A-tag linked TALER. Tx, binding site for TALERx; 5×UAS, five upstream activation sites; The blue arrow represents a minimal CMV promoter. Lines with arrows indicate up regulation and lines with bars indicate down regulation. (e) Observed data points, calculated as normalized fluorescence, on transfer curves. Each data point shows mean ± SD of fluorescent reporter from three independent replicates. (f) Transfer function curves fitted with Hill functions. n(TALERx) shows Hill coefficient that ranges from 0.51 to 1.56. (g) Nullcline analysis of TALER switches based on transfer curves fitted with Hill functions in (d), (e), (f). Solid lines represent TALER transfer curves. Dash lines represent transfer curves where OUTPUT is plotted on the horizontal axis and INPUT is plotted on the vertical axis.

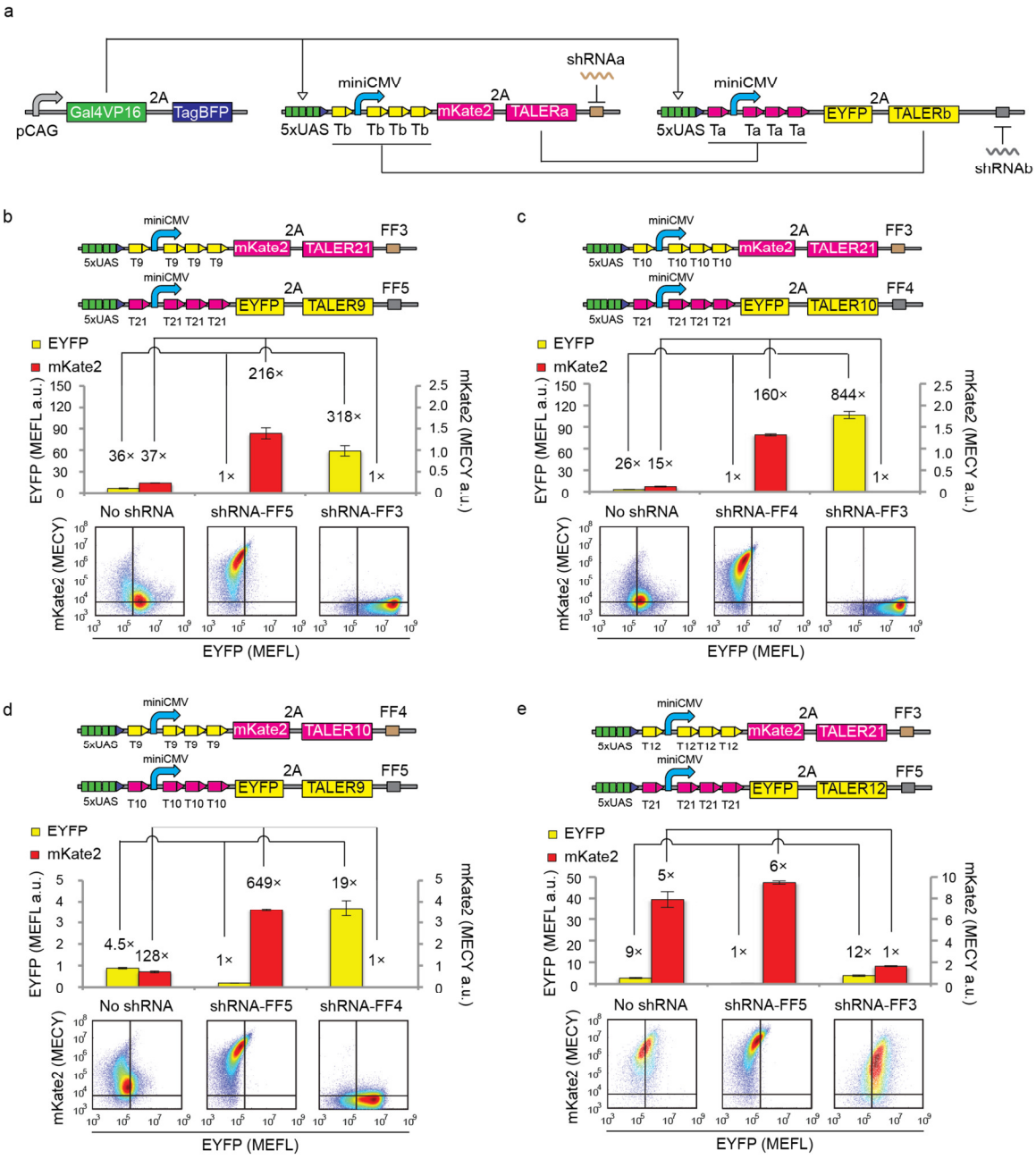
a
pCAG
Gal4VP16
2A
TagBFP
5xUAS Tb
Tb Tb Tb
miniCMV
mKate2
TALERa
shRNAa
5xUAS Ta
Ta Ta Ta
EYFP
TALERb
shRNAb
b
5xUAS T9
T9 T9 T9
FF3
TALER21
5xUAS T21
T21 T21 T21
FF5
TALER9
EYFP
mKate2
EYFP (MEFL a.u.)
mKate2 (MECY a.u.)
36× 37×
1×
216×
318×
No shRNA
shRNA-FF5
shRNA-FF3
mKate2 (MECY)
EYFP (MEFL)
c
5xUAS T10
T10 T10 T10
FF4
TALER10
26× 15×
160×
844×
shRNA-FF4
d
4.5×
128×
649×
19×
e
TALER12
T12 T12 T12
9×
5×
6×
12×

(Continued)

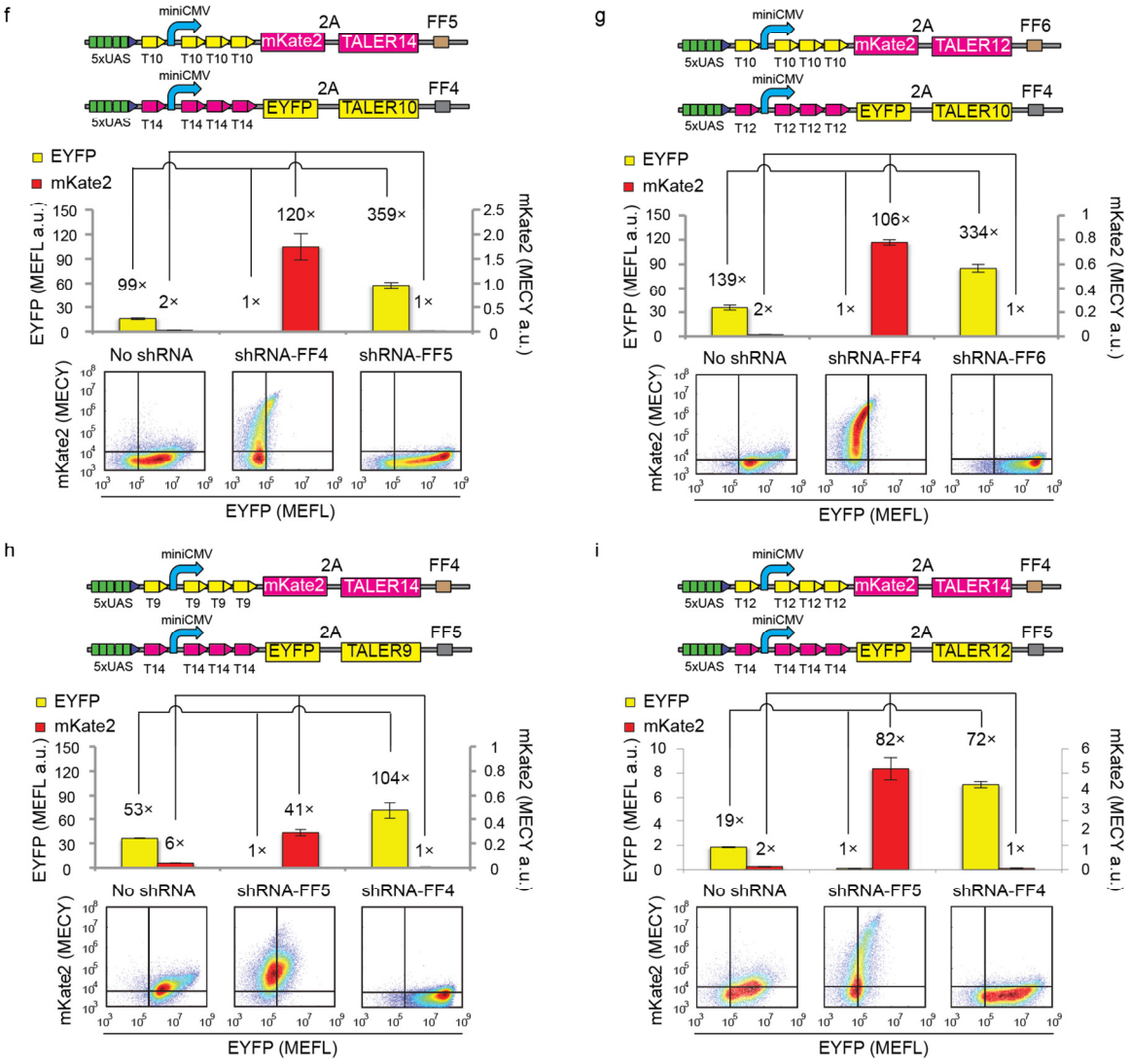

Supplementary Figure 6. Control of TALER sensory switch by using shRNAs.

(a) Circuit diagram. Each TALER is monitored by 2A-tag linked mKate2 or EYFP fluorescence. The waved lines represent shRNAs. shRNA targets are shown as a wider box. (b) to (i) Resetting TALER switch state by shRNA. The upper panel shows schematics of tested TALER sensory switches. Each bar shows mean ± SD of EYFP or mKate2 from three independent replicates. The lower panel shows representative flow cytometry scatter plots.

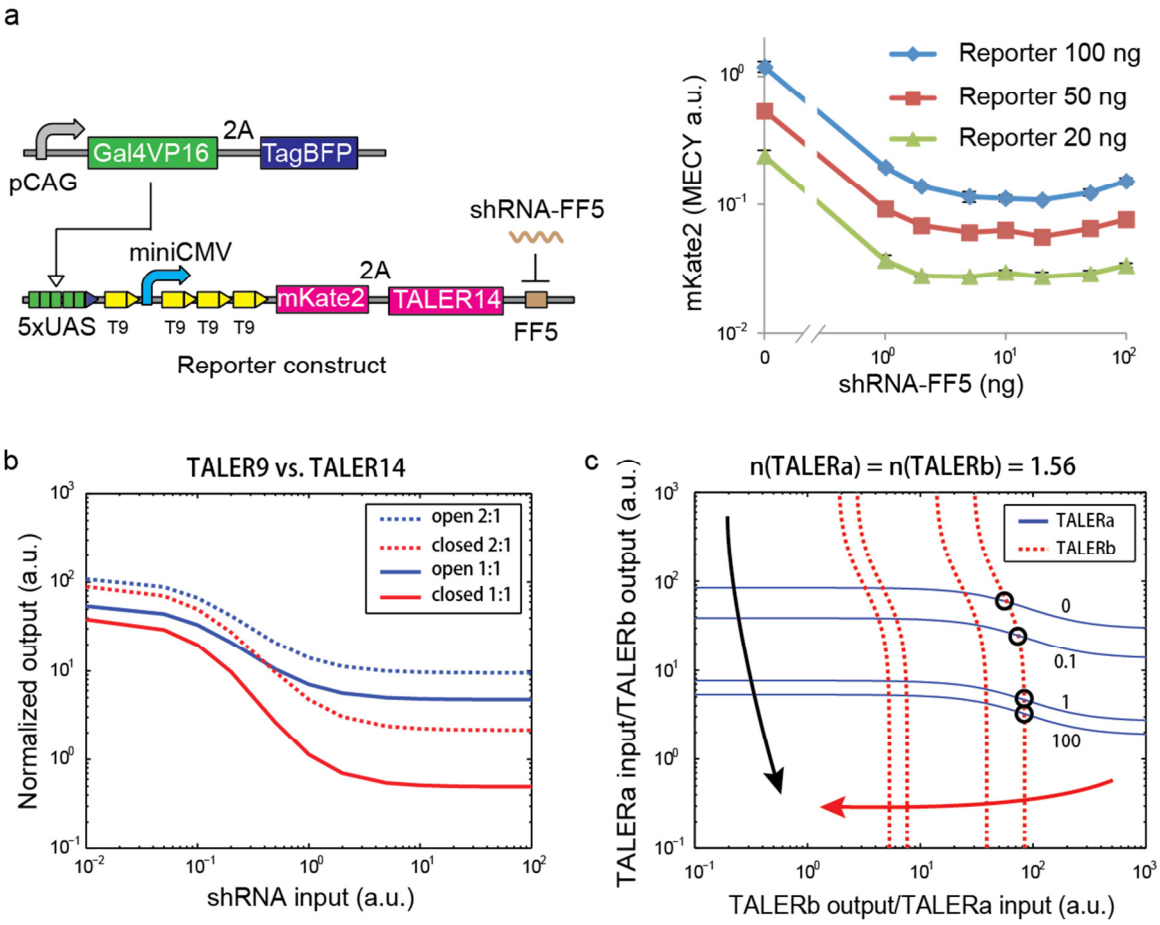

Supplementary Figure 7. Simulation of TALER sensory switches

(a) Experimentally measured knockdown of shRNA-FF5 reporter at different shRNA-FF5 doses. Three different reporter concentrations were used as indicated. (b) Simulation of closed-loop TALER switch made of TALER9 and TALER14 with mutual inhibition and the open-loop counterpart without mutual inhibition. Ratio of TALER9 to TALER14 used in simulation is indicated as 1:1 or 2:1. (c) Simulation of miRNA/shRNA regulating a TALER switch using transfer function of TALER14 and shRNA-FF5 knockdown. Hill coefficient n=1.56 is derived from TALER14. Blue solid lines represent simulated transfer functions of TALERa with 0, 0.1, 1, and 100 ng shRNA-FF5 which regulates TALERa. The black arrow indicates increasing concentrations of shRNA-FF5. Red solid lines represent simulated transfer functions of TALERb with 0, 0.1, 1 and 100 ng shRNA-FF5 which regulates TALERb. The red arrow indicates increasing concentrations of shRNA-FF5. Black circles represent the predicted equilibrium states of the switch composed of TALERb with no shRNA-FF5 and TALERa with 0, 0.1, 1 and 100 ng shRNA-FF5, respectively.

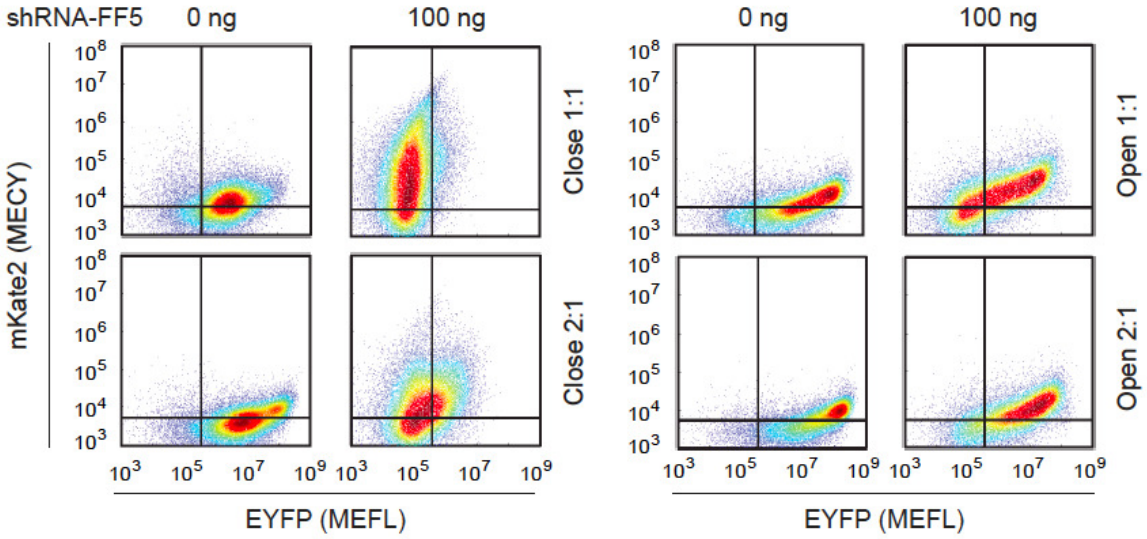

Supplementary Figure 8. Reponses of TALER sensory switches to shRNA inputs

Representative flow cytometry scatter plots measured 48 h post-transfection for indicated circuit configuration shown in Fig. 4 without shRNA or with 100 ng of shRNA. Ratio of TALER9 to TALER14 (or TALER10) used in transfection experiments is indicated as 1:1 or 2:1. Closed: closed-loop circuit; Open: open-loop circuit.

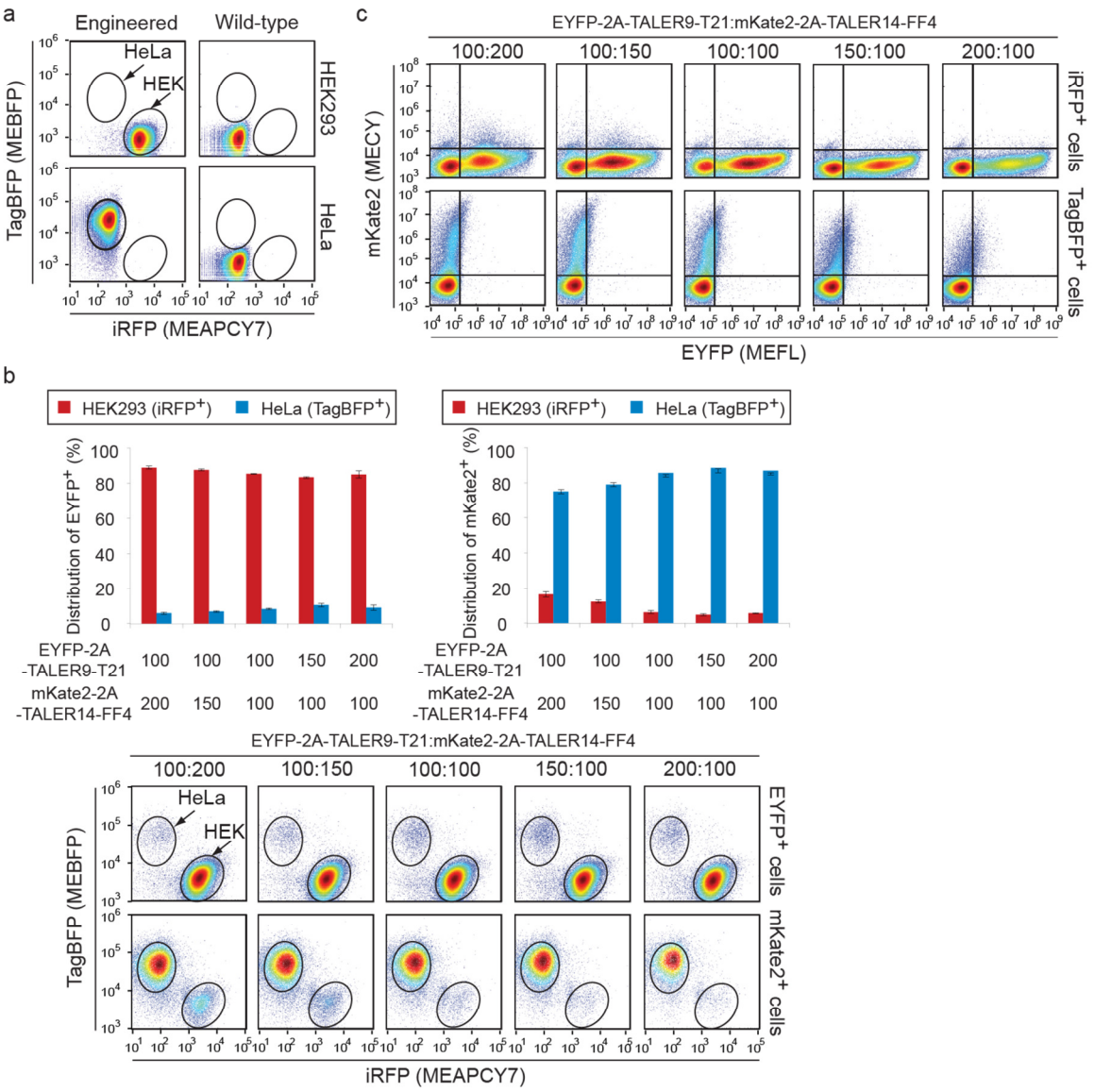

Supplementary Figure 9. Classification of engineered cell lines using microRNAs and TALER sensory switches.

(a) Scatter plots of engineered cell and wild-type HEK293 and HeLa cells. Circles represent gates for HEK293:iRFP_shRNA-FF4 and HeLa:TagBFP cells. (b) Cell classification with a TALER switch in a mixed cell population. Indicated amount of TALER DNA (ng) were used in transfection experiments. Each bar shows mean ± SD from three independent replicates. FACS data is shown in the scatter plot. The upper row shows distribution of EYFP$^+$ cells on iRFP-TagBFP scatter plots, and the lower row shows distribution of mKate2$^+$ cells on iRFP-TagBFP scatter plots. Circles indicate engineered HEK293 or HeLa cell population. (c) Representative EYFP-mKate2 scatter plots of FACS data shown in (b). Numbers on the top are ratios of two TALERs (EYFP-

2A-TALER9-T21:mKate2-2A-TALER-FF4) used in TALER switch. The upper row shows distribution of HEK293 iRFP^{+} cells on EYFP-mKate2 scatter plots, and the lower row shows distribution of HeLa TagBFP^{+} cells on EYFP-mKate2 scatter plots.

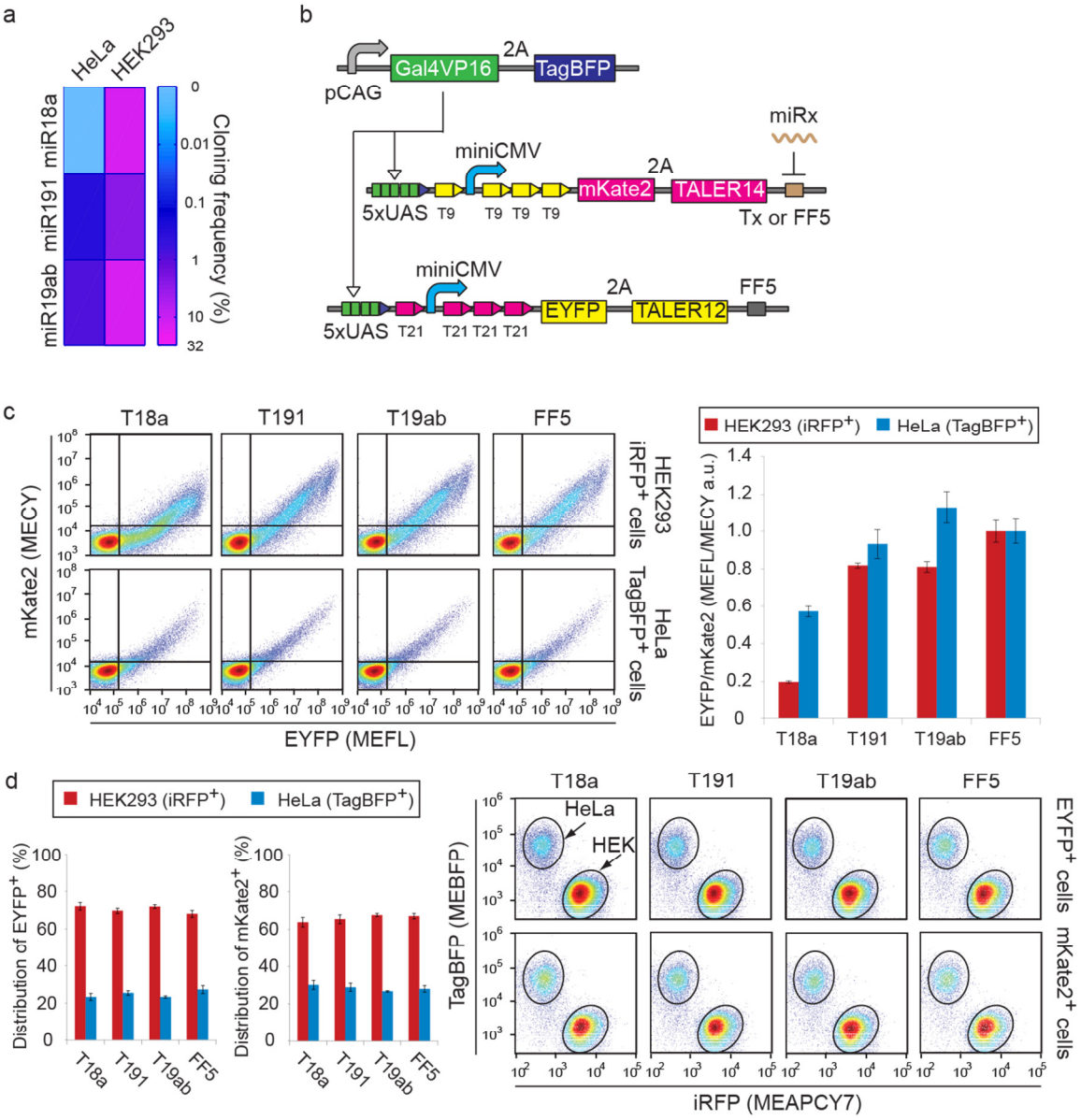

Supplementary Figure 10. Selection of HEK293-specific microRNAs in mixed cell population.

(a) Expression levels of selected microRNAs in HEK293 and HeLa cells. Cloning frequency is calculated using microRNA Atlas database[1]. MiR19ab is a combo microRNA marker that adds the expression level of both miR19a and miR19b. (b) Schematic of circuits. Each TALER is monitored by 2A-tag linked mKate2 or EYFP fluorescence. miRx, miR18a, miR191 or miR19ab. Tx or FF5, four tandem repeats of fully complementary target site for miR18a, miR191, miR19ab or shRNA-FF5. Indicated circuit was transfected into a mixed population of HEK293:iRFP_shRNA-FF4 and HeLa:TagBFP cells. (c) Left panel shows representative EYFP-mKate2 scatter plots of

HEK293 iRFP$^+$ cells and HeLa TagBFP$^+$ cells. Right panel shows microRNA knockdown efficiency in indicated cell type. Each bar shows mean of mkate2 divided by mean of EYFP from three independent replicates. (d) The bar chart in the left panel shows the fraction of engineered HEK293 and HeLa in EYFP$^+$ or mKate2$^+$ cell population. Each bar shows mean ± SD from three independent replicates. FACS scatter plots are shown in the right panel. The upper row shows distribution of EYFP$^+$ cells on iRFP-TagBFP scatter plots, and the lower row shows distribution of mKate2$^+$ cells on iRFP-TagBFP scatter plots. Circles indicate engineered HEK293 or HeLa cell population.

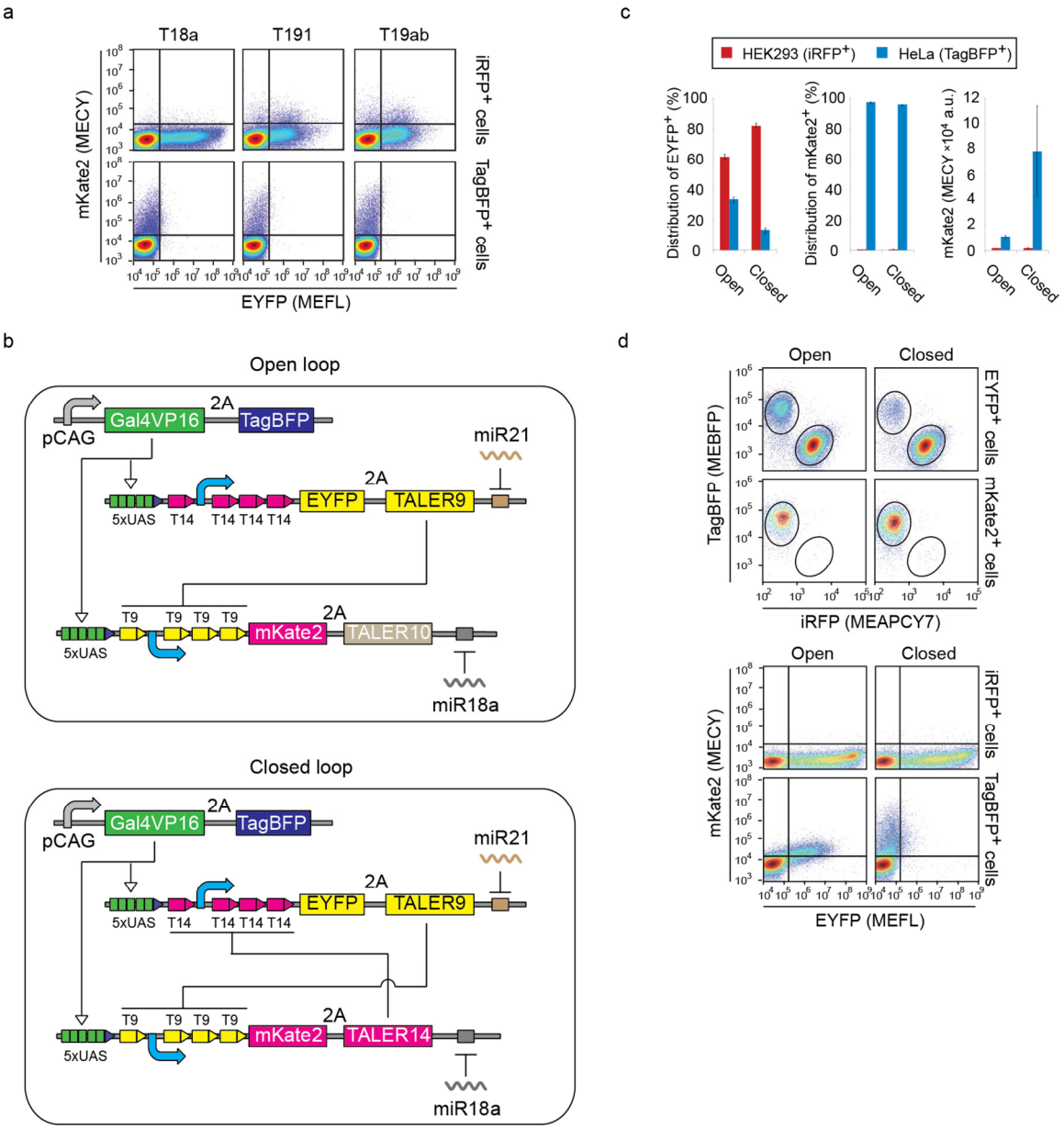

Supplementary Figure 11. Connecting endogenous microRNAs to control TALER sensory switches enables cell-type classification.

(a) Representative EYFP-mKate2 scatter plots of FACS data shown in Fig. 6c. T18a, T191 and T19ab are four tandem repeats of fully complementary target site for miR18a, miR191 and miR19ab that fused in mKate2-2A-TALER constructs, respectively. The upper row shows distribution of HEK293 iRFP$^+$ cells on EYFP-mKate2 scatter plots, and the lower row shows distribution of HeLa TagBFP$^+$ cells on EYFP-mKate2 scatter plots. (b) Schematic representation of a closed-loop TALER switch with mutual inhibition and the open-loop counterpart without mutual inhibition. Each TALER is monitored by 2A-

tag linked mKate2 or EYFP fluorescence. Four tandem repeats of fully complementary target site for miR18a or miR21 are fused in the 3'-UTR of indicated TALER constructs. Indicated circuit was transfected into a mixed population of HEK293:iRFP_shRNA-FF4 and HeLa:TagBFP cells. (c) The first two bar charts show the fraction of engineered HEK293 and HeLa in $EYFP^+$ or $mKate2^+$ cell sub-populations. The third bar chart shows the mean mKate2 values of engineered HEK293 and HeLa. Each bar shows mean ± SD from three independent replicates. (d) The upper panel shows distribution of $EYFP^+$ or $mKate2^+$ cells in iRFP-TagBFP scatter plots. Circles indicate engineered HEK293 or HeLa cell sub-populations. The lower panel shows representative EYFP-mKate2 scatter plots of HEK293 $iRFP^+$ cells and HeLa $TagBFP^+$ cells.

Supplementary Tables

Supplementary Table 1. TALER RVD sequences

TALER ID	Reference	Original ID	TALE(N) target/Organism	Length	Binding site	The position of RVD in TALER																		
						1	2	3	4	5	6	7	8	9	10	11	12	13	14	15	16	17	18	19	20	21	22	23	24
TALER1	Zhang et al.[2]	TALE1	Synthetic	14	TACGACTCACTATA	NI	HD	NN	NI	HD	NG	HD	NI	HD	NG	NI	NG	NI											
TALER2	Zhang et al.[2]	TALE4	Synthetic	14	TAAGAATAAATATA	NI	NI	NN	NI	NI	NG	NI	NI	NI	NG	NI	NG	NI											
TALER4	Zhang et al.[2]	TALE8	Synthetic	14	TACCACTCACTATA	NI	HD	HD	NI	HD	NG	HD	NI	HD	NG	NI	NG	NI											
TALER5	Cermak et al.[3]	pZHY096	SuRB/Tobacco	18	TACTGAATAATCAACACT	NI	HD	NG	NN	NI	NI	NG	NI	NI	NG	HD	NI	HD	NI	HD	NG								
TALER9	Cermak et al.[3]	pZHY106	SuRB/Tobacco	21	TATAGAACCGATCCTCCCATT	NI	NG	NI	NN	NI	NI	HD	HD	NN	NI	NG	HD	NG	HD	HD	HD	NI	NG	NG					
TALER10	Cermak et al.[3]	pZHY108	SuRB/Tobacco	20	TACCTCATCAGGAACATGTT	NI	HD	HD	NG	HD	NI	NG	HD	NI	NN	NI	HD	NG	NI	NG	NN	NG	NG					
TALER11	Cermak et al.[3]	pZHY109	SuRB/Tobacco	20	TCTTTGAAAGCCCCGCCACT	HD	NG	NG	NG	NN	NI	NI	NI	NN	HD	HD	HD	NI	HD	NI	HD	NG						
TALER12	Cermak et al.[3]	pTAL112	griblock/zebrafish	18	TATTTCGACGCTCATTCT	NI	NG	NG	NG	HD	NN	NI	HD	NN	HD	NG	HD	NI	NG	HD	NG							
TALER13	Cermak et al.[3]	pTAL117	griblock/zebrafish	17	TCCCGGAAGCCGATGCT	HD	HD	HD	NN	NN	NI	NI	NN	HD	HD	NN	NI	NG	NN	HD	NG							
TALER14	Cermak et al.[3]	grid_1116	griblock/zebrafish	17	TACCCCTCTCCGCTTCT	NI	HD	HD	HD	HD	NG	HD	NG	HD	NN	HD	NG	NG	HD	NG								
TALER15	Cermak et al.[3]	pTAL152N	white/drosophila	25	TCCTGACCATTCATCAGCCGTCTAT	HD	HD	NG	NN	NI	HD	HD	NI	NG	NG	HD	NI	NG	HD	NI	NN	HD	HD	NN	NG	HD	NG	NI	NG
TALER16	Cermak et al.[3]	pTAL153N	white/drosophila	25	TGCCCTGGGCCATCAGAAGGATCTT	NN	HD	HD	HD	HD	NN	NN	NN	HD	HD	HD	NI	NG	HD	NN	NI	NI	NN	NI	NG	HD	NG	NG	NG
TALER17	Cermak et al.[3]	pTAL162N	Plasmepsin/plasmodium	25	TATTATTGGCCTTAACCATACTCTT	NI	NG	NG	NI	NG	NG	NN	NN	HD	HD	NG	NG	NI	HD	HD	NI	NG	NI	HD	NG	HD	NG	NG	NG
TALER18	Cermak et al.[3]	pTAL163N	Plasmepsin/plasmodium	25	TCCATGTAAAACATTTTTCTGACAT	HD	HD	NI	NG	NN	NG	NI	NI	NI	HD	NI	NG	NG	NG	NG	NG	HD	NG	NN	NI	HD	NG	NI	NG
TALER19	Cermak et al.[3]	pTAL164N	TT4/arabidopsis	19	TCCATCTCCCTCAAGGATGT	HD	HD	NI	NG	HD	NG	HD	NG	HD	NI	NI	NN	NN	NI	NG	NN	NG							
TALER20	Cermak et al.[3]	pTAL165N	TT4/arabidopsis	25	TCTAGACTCTTCACAATGTTCTTAT	HD	NG	NI	NN	NI	HD	NG	HD	NG	NG	HD	NI	HD	NI	NI	NG	NN	NG	NG	HD	NG	NI	NG	
TALER21	Cermak et al.[3]	pTAL166N	TT4/arabidopsis	19	TGTCGTCTTCTGCACTTAT	NN	NG	HD	NN	NG	HD	NG	NG	HD	NG	NN	HD	NI	HD	NG	NG	NI	NG						
TALER22	Cermak et al.[3]	pTAL167N	TT4/arabidopsis	19	TAGTCAGCACCAGGCATTT	NI	NN	NG	HD	NI	NN	HD	NI	HD	HD	NI	NN	NN	HD	NI	NG	NG	NG						
TALER23	Cermak et al.[3]	pTAL69N	ADH1/arabidopsis	19	TCGGGATGCTCTCTCTAAT	HD	HD	NN	NG	NN	NI	NG	HD	NG	HD	HD	NG	HD	NG	NG	NI	NI	NG						
TALER24	Cermak et al.[3]	pTAL74N	ADH1/arabidopsis	19	TAGACAAACCACAACTCTT	NI	NN	NI	HD	NI	NI	HD	HD	HD	NI	HD	NI	NI	HD	NG	HD	NG	NG						
TALER26	Zhang et al.[2]	CAC2	Synthetic	18	TGGTAGACCTTAGGGCTA	NK	NK	NG	NI	NK	NI	HD	HD	NG	NG	NI	NK	NK	NK	HD	NG	NI							
TALER29	Zhang et al.[2]	TALE2	Synthetic	14	TCCGCCTCCCTCTC	HD	HD	NK	HD	HD	NG	HD	HD	HD	NG	HD	NG	HD											
TALER30	Zhang et al.[2]	TALE5	Synthetic	14	TATGATTTATTATA	NI	NG	NK	NI	NG	NG	NG	NI	NG	NG	NI	NG	NI											
TALER31	Zhang et al.[2]	TALE6	Synthetic	13	TAGGAGTGAGTAT	NI	NK	NK	NI	NK	NG	NK	NI	NK	NG	NI	NG												
TALER32	Zhang et al.[2]	TALE7	Synthetic	14	TACAACACACTATA	NI	HD	NI	NI	HD	NI	HD	NI	HD	NG	NI	NG	NI											
TALER35	Zhang et al.[2]	T19	Synthetic	14	TTTATTCCCTGACA	NG	NG	NI	NG	NG	HD	HD	NG	NN	NI	NG	NI												

Supplementary Table 2. Transfection configuration.

Plasmid DNA used in Figs. 1 and 2	Amount
phEF1α-TagBFP-2A-Gal4VP16-FF5	30 ng
pCMV-TALERx	200 ng
pTy+Ty+(spacing or varying binding sites)-mKate2(or dsRed)	50 ng

Plasmid DNA used in Fig. 3b and Supplementary Fig. 9	Amount
pTRE-TALERx-4xTarget^FFn	50 ng
pTRE-EBFP2	50 ng
pTx+Tx(varying binding sites)+72-mKate2	100 ng
pCAG-EYFP	50 ng
pCAG-rtTA-2A-Gal4VP16	100 ng
Final concentration of Dox	z ng/mL
z = 0, 0.1, 0.2, 0.5, 1, 2, 5, 10, 20, 50, 100, 200, 500, 1000	

Plasmid DNA used in Fig. 3e and Supplementary Fig. 9	Amount
pCAG-EYFP	50 ng
pCAG-rtTA-2A-Gal4VP16	100 ng
pTRE-EBFP2	50 ng
pTRE-TALERx-4xTarget^FFn	50 ng
pTx+Tx(varying binding sites)+72_TALERy	50 ng
pTy+Ty(varying binding sites)+72-mKate2	100 ng
Final concentration of Dox	z ng/mL
z = 0, 0.1, 0.2, 0.5, 1, 2, 5, 10, 20, 50, 100, 200, 500, 1000	

Plasmid DNA used in Fig. 4c	Amount
pTn+Tnx3+72-EYFP-2A-TALERm-4xTarget^FFx	100 ng
pTm+Tmx3+72-mKate2-2A-TALERn-4xTarget^FFy	100 ng
pCAG-Gal4VP16-2A-TagBFP-2A-Bla	100 ng

Plasmid DNA used in Fig. 4d, 4e and Supplementary Fig. 4	Amount
pTn+Tnx3+72-EYFP-2A-TALERm-4xTarget^FFx	100 ng
pTm+Tmx3+72-mKate2-2A-TALERn-4xTarget^FFy	100 ng
pCAG-Gal4VP16-2A-TagBFP-2A-Bla	100 ng
pSIREN_U6-shRNA^FFx/y-CMV-iRFP	100 ng

Plasmid DNA used in Fig. 5 ratio 1:1. Bold numbers refer to plasmid amount for ratio 2:1.	Open-loop	Closed-loop
pCAG-Gal4VP16-2A-TagBFP-2A-Bla	100 ng	100 ng
pT9+T9x3+72-mKate2-2A-TALER10-4xTarget^FF4	100 ng	
pT9+T9x3+72-mKate2-2A-TALER14-4xTarget^FF4		100 ng
pT14+T14x3+72-EYFP-2A-TALER9-4xTarget^FF5	100 (**200**) ng	100 (**200**) ng
pSIREN_U6-shRNA^FF5-CMV-iRFP	z ng	z ng
pDT7004	100-z ng	100-z ng
z = 0, 0.05, 0.1, 0.2, 0.5, 1, 2, 5, 10, 20, 50, 100		

Plasmid DNA used in Fig. 6b and Supplementary Fig. 7a	Amount
pCAG-Gal4VP16	100 ng
pT14+T14x3+72-EYFP-2A-TALER9-4xTarget^miR21	x ng
pT9+T9x3+72-mKate2-2A-TALER14-4xTarget^FF4	y ng
Final concentration of Dox	1000 ng/mL
(x:y) = (100:200), (100:150), (100:100), (150, 100), (200, 100)	

Plasmid DNA used in Fig. 6c and Supplementary Fig. 7b	Amount
pCAG-Gal4VP16	100 ng
pT9+T9x3+72-mKate2-2A-TALER14-4xTarget^miRx	100 ng
pT14+T14x3+72-EYFP-2A-TALER9-4xTarget^miR21	100 ng
Final concentration of Dox	1000 ng/mL

Plasmid DNA used in Supplementary Fig. 2a	Amount
phEF1α-rtTA-2A-Hyg-FF5	100 ng
pCAG-EYFP	100 ng
pTRE-EBFP2	100 ng
pTRE-mKate2	100 ng
Final concentration of Dox	z ng/mL
z = 0, 0.5, 1, 2, 5, 10, 20, 50, 100, 200, 500, 1000	

Plasmid DNA used in Supplementary Fig. 2b	Amount
phEF1α-rtTA-2A-Hyg-FF5	100 ng
pCAG-TagBFP	100 ng
pTRE-EYFP-2A-TALER14	100 ng
pTRE-mKate2-2A-TALER14	100 ng

Final concentration of Dox	z ng/mL
z = 0, 0.5, 1, 2, 5, 10, 20, 50, 100, 200, 500, 1000	

Plasmid DNA used in Supplementary Fig. 3	Amount
phEF1α-rtTA-2A-Hyg-FF5	100 ng
pCAG-Gal4VP16-2A-TagBFP-2A-Bla	100 ng
pTRE-EYFP-2A-TALERx-4xTarget^FFy	100 ng
pTx+Tx+72-mKate2	100 ng
Final concentration of Dox	z ng/mL
z = 0, 0.5, 1, 2, 5, 10, 20, 50, 100, 200, 500, 1000	

Plasmid DNA used in Supplementary Fig. 5a	Amount
pCAG-Gal4VP16-2A-TagBFP-2A-Bla	100 ng
pT9+T9x3+72-mKate2-2A-TALER14-4xTarget^FF5	x ng
pSIREN_U6-shRNA^FF5-CMV-iRFP	z ng
pDT7004	100-z ng
x = 20, 50, 100	
z = 0, 1, 2, 5, 10, 20, 50, 100	

Plasmid DNA used in Supplementary Fig. 6	Amount
pCAG-Gal4VP16	100 ng
pT9+T9x3+72-mKate2-2A-TALER14-4xTarget^miRx	100 ng
pT21+T21x3+72-EYFP-2A-TALER12-4xTarget^FF5	100 ng

Plasmid DNA used in Supplementary Fig. 7c and 7d	Open-loop	Closed-loop
pCAG-Gal4VP16	100 ng	100 ng
pT14+T14x3+72-EYFP-2A-TALER9-4xTarget^miR21	100 ng	100 ng
pT9+T9x3+72-mKate2-2A-TALER10-4xTarget^miRx	100 ng	
pT9+T9x3+72-mKate2-2A-TALER14-4xTarget^miRx		100 ng

Supplementary Table 3. Plasmid DNA constructs

GenBank Accession Number	Plasmid Description	GenBank Accession Number	Plasmid Description
KM486811	pCAG-VP16Gal4	KM486876	pT9+T9x3+72-mKate2-2A-TALER21-4xTarget^FF3
KM486812	pCAG-EBFP2	KM486877	pT10+T10+72-mKate2
KM486813	pCAG-EYFP	KM486878	pT10+T10x3+72-EYFP-2A-TALER9-4xTarget^FF5
KM486814	pCAG-Gal4VP16-2A-TagBFP-2A-Bla	KM486879	pT10+T10x3+72-mKate2
KM486815	pCAG-mKate2	KM486880	pT10+T10x3+72-mKate2-2A-TALER12-4xTarget^FF6
KM486816	pCAG-rtTA-2A-Gal4VP16	KM486881	pT10+T10x3+72-mKate2-2A-TALER14-4xTarget^FF4
KM486817	pCAG-TagBFP	KM486882	pT10+T10x3+72-mKate2-2A-TALER21-4xTarget^FF3
KM486818	pCMV-TALER1	KM486883	pT11+T11+72-mKate2
KM486819	pCMV-TALER2	KM486884	pT12+T12+72-mKate2
KM486820	pCMV-TALER4	KM486885	pT12+T12x3+72-EYFP-2A-TALER9-4xTarget^FF5
KM486821	pCMV-TALER5	KM486886	pT12+T12x3+72-EYFP-2A-TALER10-4xTarget^FF4
KM486822	pCMV-TALER9	KM486887	pT12+T12x3+72-mKate2
KM486823	pCMV-TALER10	KM486888	pT12+T12x3+72-mKate2-2A-TALER14-4xTarget^FF4
KM486824	pCMV-TALER11	KM486889	pT12+T12x3+72-mKate2-2A-TALER21-4xTarget^FF3
KM486825	pCMV-TALER12	KM486890	pT13+T13+72-mKate2
KM486826	pCMV-TALER13	KM486891	pT14+T14+72-mKate2
KM486827	pCMV-TALER14	KM486892	pT14+T14+72-TALER21
KM486828	pCMV-TALER15	KM486893	pT14+T14x3+72-EYFP-2A-TALER9-4xTarget^FF5
KM486829	pCMV-TALER16	KM486894	pT14+T14x3+72-EYFP-2A-TALER9-4xTarget^miR21
KM486830	pCMV-TALER17	KM486895	pT14+T14x3+72-EYFP-2A-TALER10-4xTarget^FF4
KM486831	pCMV-TALER18	KM486896	pT14+T14x3+72-EYFP-2A-TALER12-4xTarget^FF5
KM486832	pCMV-TALER19	KM486897	pT14+T14x3+72-mKate2
KM486833	pCMV-TALER20	KM486898	pT14+T14x3+72-mKate2-2A-TALER21-4xTarget^FF3
KM486834	pCMV-TALER21	KM486899	pT14+T14x3+72-TALER21
KM486835	pCMV-TALER22	KM486900	pT15+T15+72-mKate2
KM486836	pCMV-TALER23	KM486901	pT16+T16+72-mKate2
KM486837	pCMV-TALER24	KM486902	pT17+T17+72-mKate2
KM486838	pCMV-TALER26	KM486903	pT18+T18+72-mKate2
KM486839	pCMV-TALER29	KM486904	pT19+T19+72-mKate2

KM486840	pCMV-TALER30	KM486905	pT20+T20+72-mKate2
KM486841	pCMV-TALER31	KM486906	pT21+T21+72-mKate2
KM486842	pCMV-TALER32	KM486907	pT21+T21+72-TALER14
KM486843	pCMV-TALER35	KM486908	pT21+T21x3+72-EYFP-2A-TALER14-4xTarget^FF4
KM486844	phEF1α-EYFP-2A-Hyg	KM486909	pT21+T21x3+72-EYFP-2A-TALER9-4xTarget^FF5
KM486845	phEF1α-rtTA-2A-Hyg-FF5	KM486910	pT21+T21x3+72-EYFP-2A-TALER10-4xTarget^FF4
KM486846	phEF1α-TagBFP-2A-Gal4VP16-FF5	KM486911	pT21+T21x3+72-EYFP-2A-TALER12-4xTarget^FF5
KM486847	pSIREN_U6-shRNA^FF3-CMV-iRFP	KM486912	pT21+T21x3+72-mKate2
KM486848	pSIREN_U6-shRNA^FF4-CMV-iRFP	KM486913	pT21+T21x3+72-TALER14
KM486849	pSIREN_U6-shRNA^FF5-CMV-iRFP	KM486914	pT22+T22+72-mKate2
KM486850	pSIREN_U6-shRNA^FF6-CMV-iRFP	KM486915	pT23+T23+72-mKate2
KM486851	pT1+T1+72-DsRed	KM486916	pT24+T24+72-mKate2
KM486852	pT1+T1+72-mKate2	KM486917	pT26+T26+72-mKate2
KM486853	pT1+T2+72-DsRed	KM486918	pT29+T29+72-mKate2
KM486854	pT1+T1+78-mKate2	KM486919	pT30+T30+72-mKate2
KM486855	pT1+T1+83-mKate2	KM486920	pT31+T31+72-mKate2
KM486856	pT1+T1+89-mKate2	KM486921	pT32+T32+72-mKate2
KM486857	pT1+T1+94-mKate2	KM486922	pT32+T32x3+72-mKate2
KM486858	pT1+T1+100-mKate2	KM486923	pT35+T35+72-mKate2
KM486859	pT2+T1+72-DsRed	KM486924	pTRE-EBFP2
KM486860	pT2+T2+72-DsRed	KM486925	pTRE-EYFP
KM486861	pT2+T2+72-mKate2	KM486926	pTRE-EYFP-2A-TALER9-4xTarget^FF5
KM486862	pT2+T2x3+72-mKate2	KM486927	pTRE-EYFP-2A-TALER10-4xTarget^FF4
KM486863	pT4+T4+72-mKate2	KM486928	pTRE-EYFP-2A-TALER12-4xTarget^FF5
KM486864	pT4+T4x3+72-mKate2	KM486929	pTRE-EYFP-2A-TALER14-4xTarget^FF4
KM486865	pT5+T5+72-mKate2	KM486930	pTRE-EYFP-2A-TALER21-4xTarget^FF5
KM486866	pT5+T5x3+72-mKate2	KM486931	pTRE-mKate2
KM486867	pT9+T9+72-mKate2	KM486932	pTRE-mKate2-2A-TALER14
KM486868	pT9+T9x3+72-mKate2	KM486933	pTRE-TALER14-4xTarget^FF4
KM486869	pT9+T9x3+72-mKate2-2A-TALER10-4xTarget^FF4	KM486934	pTRE-TALER21-4xTarget^FF3
KM486870	pT9+T9x3+72-mKate2-2A-TALER12-4xTarget^FF6	KM519784	pT9+T9x3+72-mKate2-2A-TALER10-4xTarget^FF5
KM486871	pT9+T9x3+72-mKate2-2A-TALER14-4xTarget^FF4	KM519785	pT9+T9x3+72-mKate2-2A-TALER10-4xTarget^T18a

KM486872	pT9+T9x3+72-mKate2-2A-TALER14-4xTarget^FF5	KM519786	pTRE-mKate2-2A-TALER12-4xTarget^FF4
KM486873	pT9+T9x3+72-mKate2-2A-TALER14-4xTarget^T18a	KM519787	pH1TO-hEF1α-TetR-2A-TagBFP-2A-Bla
KM486874	pT9+T9x3+72-mKate2-2A-TALER14-4xTarget^T19ab	KM519788	pH1TO-shRNA^FF4-hEF1α-TetR-2A-iRFP-2A-Bla
KM486875	pT9+T9x3+72-mKate2-2A-TALER14-4xTarget^T191		

Supplementary Table 4. Minimal Hamming distance between TALER binding sites and genomic sequences of genes differentially expressed

Experiment:	Hygro-T09 and TALER10-T10
DE gene	Minimal Hamming distance
AHNAK	6
BACE1-AS	8
CAMKMT	4
DNAJB1	8
GOPC	5
KLC1	6
SIRT7	6
SLMO2-ATP5E	6
SNAR-C3	7
STK10	5
ZNF613	7

Experiment:	Hygro-T09 and TALER12-T12
DE gene	Minimal Hamming distance
ANKHD1	5
ATXN7L2	6
C14orf169	5
C20orf96	6
C6orf203	6
CAND1	5
CAPG	6
CCRN4L	5
CDC45	5
GLT8D1	6
GRB2	5
HIST2H4A	7
HIST2H4B	7
LOC642846	5
NAB2	6
NUP153	5

PI4KAP2	5
RNF2	5
SLC27A3	6
SMA4	3
SNAR-C3	6
STAG3L3	5
TCEAL7	6
UBXN8	6
ZFP36L2	6

Experiment:	Hygro-T09 and TALER14-T14
DE gene	Minimal Hamming distance
CCDC51	5
GLUD1	4
GSTO2	4
LMNB2	4
NUDT6	5
RAC1	5
RASSF4	4
RHOT1	5
SPRTN	5
XXYLT1	3

Supplementary References:

1. Landgraf, P. et al. A mammalian microRNA expression atlas based on small RNA library sequencing. *Cell* **129**, 1401-1414 (2007).

2. Zhang, F. et al. Efficient construction of sequence-specific TAL effectors for modulating mammalian transcription. *Nat Biotechnol* **29**, 149-153 (2011).

3. Cermak, T. et al. Efficient design and assembly of custom TALEN and other TAL effector-based constructs for DNA targeting. *Nucleic Acids Res* **39**, e82 (2011).